Current-mediated synchronization of a pair of beating non-identical flagella

V S Dotsenko, A Maciolek, G. Oshanin, O Vasilyev, S Dietrich

PAPER • OPEN ACCESS

Current-mediated synchronization of a pair of beating non-identical flagella

New Journal of Physics
The open access journal at the forefront of physics

Deutsche Physikalische Gesellschaft DPG
IOP Institute of Physics

Published in partnership with: Deutsche Physikalische Gesellschaft and the Institute of Physics

OPEN ACCESS

RECEIVED
7 January 2019

REVISED
4 February 2019

ACCEPTED FOR PUBLICATION
26 February 2019

PUBLISHED
28 March 2019

PAPER

Current-mediated synchronization of a pair of beating non-identical flagella

V S Dotsenko[1,2], **A Maciolek**[3,4,5], **G Oshanin**[1,3], **O Vasilyev**[3,4] and **S Dietrich**[3,4]

[1] Sorbonne Université, CNRS, Laboratoire de Physique Théorique de la Matière Condensée, LPTMC (UMR CNRS 7600), F-75252 Paris Cedex 05, France
[2] LD Landau Institute for Theoretical Physics, 119334 Moscow, Russia
[3] Max-Planck-Institut für Intelligente Systeme, Heisenbergstraße 3, D-70569 Stuttgart, Germany
[4] IV Institut für Theoretische Physik, Universität Stuttgart, D-70569 Stuttgart, Germany
[5] Institute of Physical Chemistry, Polish Academy of Sciences, Department III, Kasprzaka 44/52, PL-01-224 Warsaw, Poland

E-mail: oshanin@lptmc.jussieu.fr

Keywords: out-of-equilibrium systems, synchronization, single-trajectory analysis, ensemble-averaged properties, noise in biological systems

Abstract

The basic phenomenology of experimentally observed synchronization (i.e. a stochastic phase locking) of identical, beating flagella of a biflagellate alga is known to be captured well by a minimal model describing the dynamics of coupled, limit-cycle, noisy oscillators (known as the noisy Kuramoto model). As demonstrated experimentally, the amplitudes of the noise terms therein, which stem from fluctuations of the rotary motors, depend on the flagella length. Here we address the conceptually important question which kind of synchrony occurs if the two flagella have different lengths such that the noises acting on each of them have different amplitudes. On the basis of a minimal model, too, we show that a different kind of synchrony emerges, and here it is mediated by a current carrying, steady-state; it manifests itself via correlated 'drifts' of phases. We quantify such a synchronization mechanism in terms of appropriate order parameters Q and $Q_{\mathcal{S}}$—for an ensemble of trajectories and for a single realization of noises of duration $\mathcal{S}$, respectively. Via numerical simulations we show that both approaches become identical for long observation times $\mathcal{S}$. This reveals an ergodic behavior and implies that a single-realization order parameter $Q_{\mathcal{S}}$ is suitable for experimental analysis for which ensemble averaging is not always possible.

1. Introduction

There is experimental evidence that two beating flagella, extending from one end of the biflagellate alga *Chlamydomonas* reinhardtii, synchronize their dynamics. Analyzing the oscillatory intensity signals $x_{1,2}(t) = \Gamma_{1,2}(t)\sin(2\pi\theta_{1,2}(t))$ (where $\Gamma_{1,2}(t)$ and $\theta_{1,2}(t)$ are the amplitudes and the instantaneous phases of the periodic motion of flagella 1 and 2, respectively), which are obtained by local sampling of the video light intensity near the two flagella, Polin *et al* [1] observed that the phase difference $\triangle_t = \theta_1(t) - \theta_2(t)$ contains periods of synchrony (i.e. the so-called phase locking behavior with $\Delta_t \approx$ const [2–5]), interrupted by sudden drifts of either sign. Referring to earlier ideas, that the hydrodynamic interactions between eukaryotic flagella or cilia may underlie their synchronization [6–13], Goldstein *et al* [14] proposed a phenomenological, minimal, stochastic model in which the motion of a flagella pair is described by two noisy phase oscillators which move on circular trajectories and are coupled via an antisymmetric function of the phase difference $\triangle_t$. In terms of the notations used in [14], the equations of motion read

$$\begin{aligned}\dot{\theta}_1(t) &= \nu_1 + \pi\varepsilon\sin[2\pi(\theta_2(t) - \theta_1(t))] + \zeta_1(t),\\ \dot{\theta}_2(t) &= \nu_2 + \pi\varepsilon\sin[2\pi(\theta_1(t) - \theta_2(t))] + \zeta_2(t).\end{aligned} \tag{1}$$

In equation (1), the dimensionless functions $\theta_{1,2}(t) \in (-1/2, 1/2)$ are the two phases mentioned above, the dot denotes the time derivative, ν_1 and ν_2 are the natural frequencies (Hz) of the flagella 1 and 2, respectively, and ε

(Hz) is the amplitude of the coupling between the flagella. This phenomenological parameter accounts for the fact that fluid flows driven by beating flagella provide a hydrodynamic coupling between the latter. Lastly, $\zeta_{1,2}(t)$ are delta-correlated, Gaussian white noises with zero mean and identical covariances[6] [15]: $\overline{\zeta_i(t)\zeta_j(t')} = 2T_{\rm eff}\,\delta_{i,j}\delta(t-t')$, where the bar denotes the average over realizations of the noises; $i, j \in 1,2$; $\delta_{i,j}$ is the Kronecker symbol while $T_{\rm eff}$ (Hz) can be considered as an *effective* 'temperature', because it defines the amplitude of the noise terms. Importantly, the major contribution to $T_{\rm eff}$ stems from the fluctuations of the rotary motors of flagella [14, 16, 17]. Indeed, these *active* fluctuations are several orders of magnitude larger than the thermal noise [14, 17], so that the flagella are not in thermal equilibrium with its bath.

We note that the sine terms in equation (1), which link the time evolutions of $\theta_1(t)$ and $\theta_2(t)$, describe the actual coupling due to hydrodynamic interactions between the two flagella [6–13] only in an effective way. However, up to now no other good and justified alternative to such a phenomenological description has emerged. In particular, explicit results presented in, e.g. [13], are based on the assumption that the distance between the two flagella is much larger than their length, which is not the case for the system studied in [14]. We also note that in more complex situations of unicellular algal species bearing *multiple* flagella, both the effective coupling introduced in [14] and the results in [6–13] may turn out to be insufficient to describe properly all facets of the synchronized behavior: a different synchronization scenario may be realized which is provided, e.g. by contractile fibers of the basal apparatus [18, 19].

Solving equation (1) numerically for given realizations of the noise terms, Goldstein *et al* [14] have found consistency between Δ_t evolving according to equation (1) and the experimentally observed behavior of the flagella of the biflagellate alga [1], i.e. the calculated trajectories of the phase difference exhibit essentially the same noisy synchronization interrupted by occasional phase slips.

The comparison with experimental data has facilitated to identify the physically relevant values of the parameters entering the effective Langevin equations. In particular, for flagella of length $l \simeq 12\ \mu$m, observations based on the dynamics of 21 individuals and the comparison with the time series for Δ_t, spanning over an interval of 10^2 s (i.e. containing several thousands of beats), have shown that ε lies within the range 0.14–0.7 Hz and that the effective temperature $T_{\rm eff}$ is within the range 0.05–0.28 Hz, while $\nu = (\nu_1 + \nu_2)/2 \simeq 47$ Hz and $\delta\nu/\nu = |\nu_1 - \nu_2|/\nu \simeq 0.004$. The experimentally obtained values of ε appear to be in line with the theoretical prediction in [13]. Importantly, the results of [14] have emphasized for the first time the essential role played by the biochemical noise in the dynamics of eukaryotic flagella as manifested by its realization-to-realization fluctuations.

A more sophisticated experimental analysis has been performed in [20], which is focused on the dependence of the coupling parameter ε and of the effective temperature $T_{\rm eff}$ on the length l of the flagella. This enhanced experimental analysis took advantage of the ability of the *Chlamydomonas* reinhardtii alga to shed its flagella and to regrow them after a deflagellation has occurred [21]. The flagella of length $l \simeq 10.82\ \mu$m have been first clipped by a micropipette [20] and then left to regrow. Within 90 min the flagella reached the length $l \simeq 11.48\ \mu$m, which, surprisingly, exceeded the original one. The dynamics of the slowly growing flagella has been recorded every ten minutes within time intervals two minutes long (within which the length of the flagella did not appreciably change).

From 19 such experiments it was inferred [20] that, for progressively longer flagella, the periods of the synchronous beating of both flagella become more pronounced. Analyzing the data, it was shown that, as the flagella grow, the beating frequency ν decreases $\propto 1/l$, implying that the beating mechanism operates at constant power output per length (see [20]). The coupling parameter ε turned out to be linearly proportional to l, which explains the trend for a progressive increase of the synchronization periods. Therefore, the proportionality $\varepsilon \propto l$ is in agreement with the elastohydrodynamic scaling $\varepsilon \propto \nu^2 l^3$ as predicted in [13]. Lastly, a variation of $T_{\rm eff}$ with l has been observed. In particular, for $l \simeq 6\ \mu$m, $T_{\rm eff}$ was found to lie within the range 0.06–0.09 Hz, while for $l \simeq 8\ \mu$m it lies within the range 0.04–0.06 Hz, which is not overlapping with the previous interval. For larger values of l, $T_{\rm eff}$ was shown to saturate at a constant value of the order of 0.04 Hz. Therefore, $T_{\rm eff}$ evidently depends on l, at least for sufficiently short flagella, such that it is larger for shorter flagella. In view of the active nature of the fluctuations of the rotary motors, this is in line with the intuitively expected behavior[7].

Once noise appears to be a physically relevant parameter, it is natural to explore a wider range of possible effects. In this sense the conceptually important question arises what kind of synchronization, if any, may take place in situations in which the length of the two flagella differ. Such a situation may apparently be realized experimentally by amputating just one flagellum of the biflagellate alga, and by leaving the second one intact, as described in [21]. We note that in this case the regeneration scenario is more complicated, as compared to the

[6] Note that the definition of the covariance of the noise terms used in [14] does not contain the usual prefactor 2 of the temperature (see, e.g. [15]). Thus, in our settings $T_{\rm eff}$ is half the analogous quantity in [14]. The values of $T_{\rm eff}$, which we present in the main text, take this property into account.

[7] We note that the amplitude of the noise of a single flagellum as a function of its length l might be different from that inferred from the experimental data in [20] for a pair of flagella.

case when both flagella are removed (see [20]). Here, the intact flagellum first shortens linearly in time while the amputated one regenerates. This way the two flagella attain an equal, intermediate length. Then both grow and eventually approach their initial length at the same rate. However, the time required to reach an equal intermediate length can be quite long, i.e. 20–40 min [21]. It can become even longer if certain chemicals (e.g. colchicine) are added after a deflagellation, which inhibit the regeneration process [21, 22]. Therefore, there is a time window in which both flagella have distinctly different lengths. Within this time window, the coupled phases $\theta_1(t)$ and $\theta_2(t)$ will undergo a stochastic evolution—each at its own temperature $T_{\rm eff}^{(1)}$ or $T_{\rm eff}^{(2)}$, respectively. Such a system is no longer characterized by a unique effective temperature $T_{\rm eff}$. One expects that the Fokker–Planck equation [15] associated with the Langevin equations (1) will have a non-trivial, current-carrying steady-state solution. In the following we shall refer to the case of unequal temperatures as an out-of-equilibrium case, keeping in mind, of course, that the original physical system is not in equilibrium with its bath, even for $T_{\rm eff}^{(1)} = T_{\rm eff}^{(2)}$.

Viewed from a different perspective, which is perhaps equally important due to certain other applications (see [24] for a discussion) we note that the minimal model in equation (1) with a unique effective temperature $T_{\rm eff}$ represents the so-called Sakaguchi model [25] which is a noisy version of the celebrated Kuramoto model of coupled oscillators (see, e.g. [2–5]). Its generalization to the case of two different temperatures[8] emerges naturally within the present context of the synchronization of beating, non-identical flagella. We note parenthetically that recently the stochastic evolution of systems with several temperatures was intensively studied and a wealth of interesting out-of-equilibrium phenomena has been predicted (see, e.g. [26–33] and references therein). To the best of our knowledge, the issue of synchronization under out-of-equilibrium conditions in general, and in a system with two degrees of freedom exposed to two different effective temperatures in particular, has not yet been addressed. Inter alia, this motivates our quest for synchrony in a minimal model with two different effective temperatures.

Here, we focus on the stochastic evolution of the phases $\theta_1(t)$ and $\theta_2(t)$ of two coupled oscillators, which obeys the minimal model in equation (1) with the covariance functions of the noise terms of the form

$$\overline{\zeta_i(t)\zeta_j(t)} = 2\,\delta_{i,j}\,T_{\rm eff}^{(i)}\,\delta(t-t'),\quad i,j=1,2, \tag{2}$$

where $T_{\rm eff}^{(1)}$ and $T_{\rm eff}^{(2)}$ are, in general, not equal. For simplicity, we assume that the natural frequencies of both oscillators are the same, $\nu_1 = \nu_2 = \nu$. On one hand, this assumption appears to be justified because the experimentally observed difference of the natural frequencies is indeed rather small (see above) [14], so that in a first approximation it can be neglected. On the other hand, this assumption allows us to disentangle the effects of an out-of-equilibrium active noise from the effects caused by a possible, albeit small, difference of the natural frequencies ν_1 and ν_2.

We demonstrate, both analytically and numerically, that in such a system an emerging steady-state is characterized by a nonzero current $j(\theta_1, \theta_2)$ in the frame of reference rotating with frequency ν (note that $j(\theta_1, \theta_2) \equiv 0$ when $T_{\rm eff}^{(1)} = T_{\rm eff}^{(2)}$). This current, which is the same for both phases, with an amplitude depending on the instantaneous values of $\theta_1(t)$ and $\theta_2(t)$, sustains a synchronized time evolution of the rates $\dot\theta_1(t)$ and $\dot\theta_2(t)$ at which the phases change, i.e. it produces correlated drifts of phases. At the same time, we realize that the stochastic phase locking seen in [14] degrades for unequal effective temperatures (see figure 1) and is weakest in the case that one of the effective temperatures equals zero, i.e. that the corresponding rotary motor does not fluctuate. In order to quantify the degree of synchronization, based on the correlated drifts of phases, we define a characteristic order parameter Q, which measures the relative amount of the novel, out-of-equilibrium synchronization mechanism and vanishes if the effective temperatures of the noise terms become equal. This definition of Q is based on the explicit expression derived here for the steady-state current $j(\theta_1, \theta_2)$ and hence, it represents a property averaged over the statistical ensemble of the trajectories of $\theta_1(t)$ and $\theta_2(t)$. In experiments, however, it is often not possible to garner a sufficiently large statistical sample in order to carry out this kind of averaging. For this reason, we propose an analogous order parameter $Q_{\mathcal{S}}$ defined on the level of a single-realization of the trajectories $\theta_1(t)$ and $\theta_2(t)$ tracked within a time interval $(0,\ \mathcal{S})$. We show, via numerical simulations, that both definitions lead to consistent results, i.e. $Q_{\mathcal{S}} \to Q$ in the limit of an unlimited long observation time $\mathcal{S}$. This result, inter alia, shows that the system under study is ergodic, which cannot be expected *a priori*, especially if $T_{\rm eff}^{(1)} \neq T_{\rm eff}^{(2)}$.

The outline of the paper is as follows. In section 2 we present our main results obtained for the model defined by equations (1) and (2). We present here explicit expressions for the probability density function (pdf) in the steady-state, the steady-state current and an ensemble-averaged order parameter. Further on, we introduce analogous quantities for individual realizations of $\theta_1(t)$ and $\theta_2(t)$. In section 3 we discuss the behavior of the ensemble-averaged quantities and of their counterparts defined for a single realization of noises, and outline

[8] The dynamics of two coupled Kuramoto oscillators exposed to two unequal noises has been already studied (see [3, 23, 24]). However, for this situation the only (albeit quite complicated) issue, which was considered, concerns the form of the diffusion coefficient of the phase difference Δ_t.

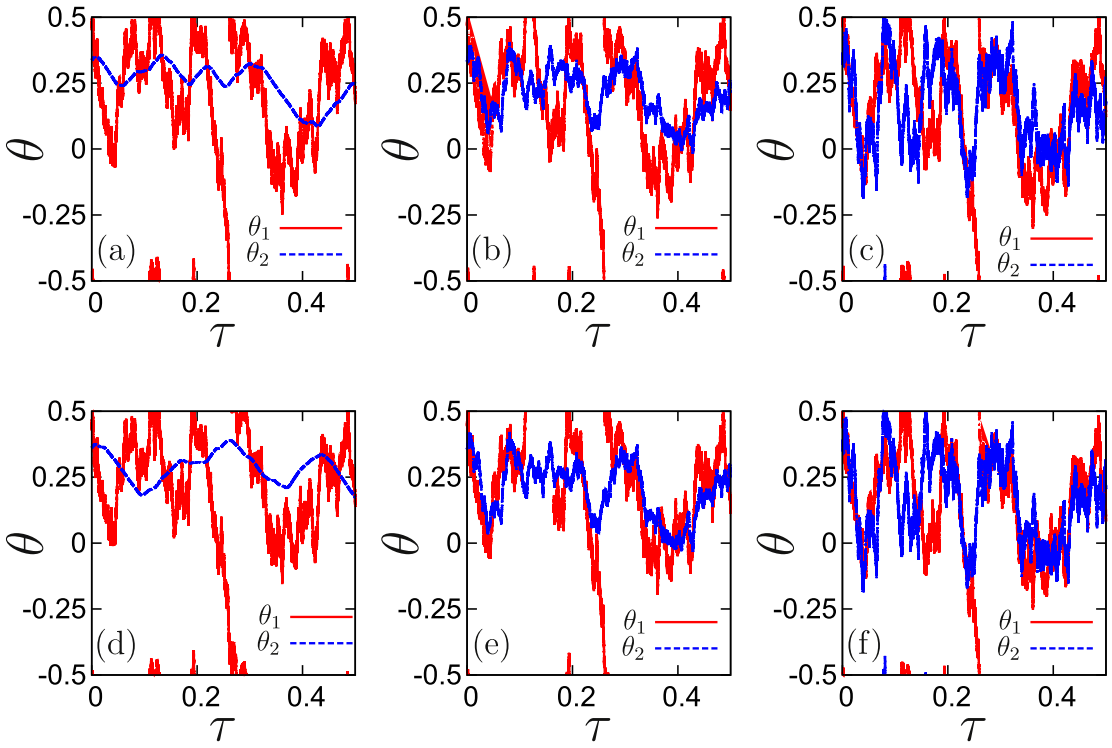

Figure 1. Individual realizations of (short) trajectories $\theta_1(t)$ and $\theta_2(t)$ (recall that $\theta_1(t), \theta_2(t) \in (-1/2, 1/2)$ are periodic quantities), defined in the reference frame rotating with the frequency ν, for $T_{\rm eff}^{(1)} = 0.5$ Hz as functions of the reduced, dimensionless time $\tau = T_{\rm eff}^{(1)}\, t$. The observation time is $\mathcal{S} = 1$ s only. Panel (a): $\varepsilon = 0.5$ Hz and $T_{\rm eff}^{(2)} = 0$, i.e. the rotary motor of the second flagellum is perfect in that it does not fluctuate. Panel (b): $\varepsilon = 0.5$ Hz and $T_{\rm eff}^{(2)} = 0.1$ Hz. Panel (c): $\varepsilon = 0.5$ Hz and $T_{\rm eff}^{(2)} = 0.5$ Hz. Panel (d): $\varepsilon = 1$ Hz and $T_{\rm eff}^{(2)} = 0$. Panel (e): $\varepsilon = 1$ Hz and $T_{\rm eff}^{(2)} = 0.1$ Hz. Panel (f): $\varepsilon = 1$ Hz and $T_{\rm eff}^{(2)} = 0.5$ Hz. The individual trajectories $\theta_1(t)$ and $\theta_2(t)$ exhibit a noisy dynamics, but nonetheless evolve alongside each other for rather extended periods of time. This is precisely the stochastic phase locking phenomenon described in [14] for the case of equal temperatures. It is inferred by following the time evolution of the phase difference $\Delta_t = \theta_1(t) - \theta_2(t)$ in experiments and in numerical simulations. Here, we observe that this kind of stochastic synchronization [14] degrades if $T_{\rm eff}^{(1)} \neq T_{\rm eff}^{(2)}$. Indeed, the stochastic phase locking is seemingly strongest in the case of equal temperatures (panels (c) and (f)). It is less pronounced for the combination $T_{\rm eff}^{(1)} = 0.5$ Hz and $T_{\rm eff}^{(2)} = 0.1$ Hz (panels (b) and (e)), and it is weakest for $T_{\rm eff}^{(1)} = 0.5$ Hz and $T_{\rm eff}^{(2)} = 0$ (panels (a) and (d)), for which the periods of synchronization in the dynamics of $\theta_1(t)$ and $\theta_2(t)$ are hardly visible.

some perspectives for future research. Details of calculations are relegated to the appendix. Here, we provide the Fokker–Planck equation associated with the minimal Langevin model in equations (1) and (2), and present its solution in the limit $t \to \infty$. We also describe our numerical approach, which is based on the discretization of the Langevin equations in equation (1).

2. Results

2.1. Ensemble-averaged properties

2.1.1. Pdf in the steady state

Our main analytical result is an exact expression for the joint pdf $P(\theta_1, \theta_2)$, which is the steady-state solution of the Fokker–Planck equation (see equation (A1) in the appendix) associated with a system of two coupled Langevin equations (equation (1)), and with the noise terms defined by equation (2):

$$P(\theta_1,\, \theta_2) = \frac{1}{Z} \exp\left(\frac{\varepsilon}{2\overline{T}_{\rm eff}} \cos\left(2\pi(\theta_1 - \theta_2)\right) \right), \tag{3}$$

where $\overline{T}_{\rm eff}$ is the 'mean' effective temperature[9] $\overline{T}_{\rm eff} = (T_{\rm eff}^{(1)} + T_{\rm eff}^{(2)})/2$, while Z insures that $P(\theta_1, \theta_2)$ is properly normalized, i.e. $\int_{-1/2}^{1/2} \int_{-1/2}^{1/2} {\rm d}\theta_1 {\rm d}\theta_2 P(\theta_1,\, \theta_2) = 1$. This normalization constant can be calculated exactly and is

[9] The effective temperatures enter the steady-state pdf in equation (3) only in an additive way, such that there is no singular behavior in the case that they are unequal; here the only pertinent quantity is the mean effective temperature $\overline{T}_{\rm eff}$. We note that this seems to be a general rule (see equation (3) in [28]) for any form of the coupling term between the phases $\theta_1(t)$ and $\theta_2(t)$ in equation (1), which depends on the phase difference only. As a consequence, the standard complex order parameter $r\, \exp({\rm i}\Psi) \equiv (\exp(2\pi {\rm i}\theta_1) + \exp(2\pi {\rm i}\theta_2))/2$, where r defines the phase coherence and Ψ the average phase [2, 4, 5], averaged over the pdf given in equation (3), is exactly equal to zero.

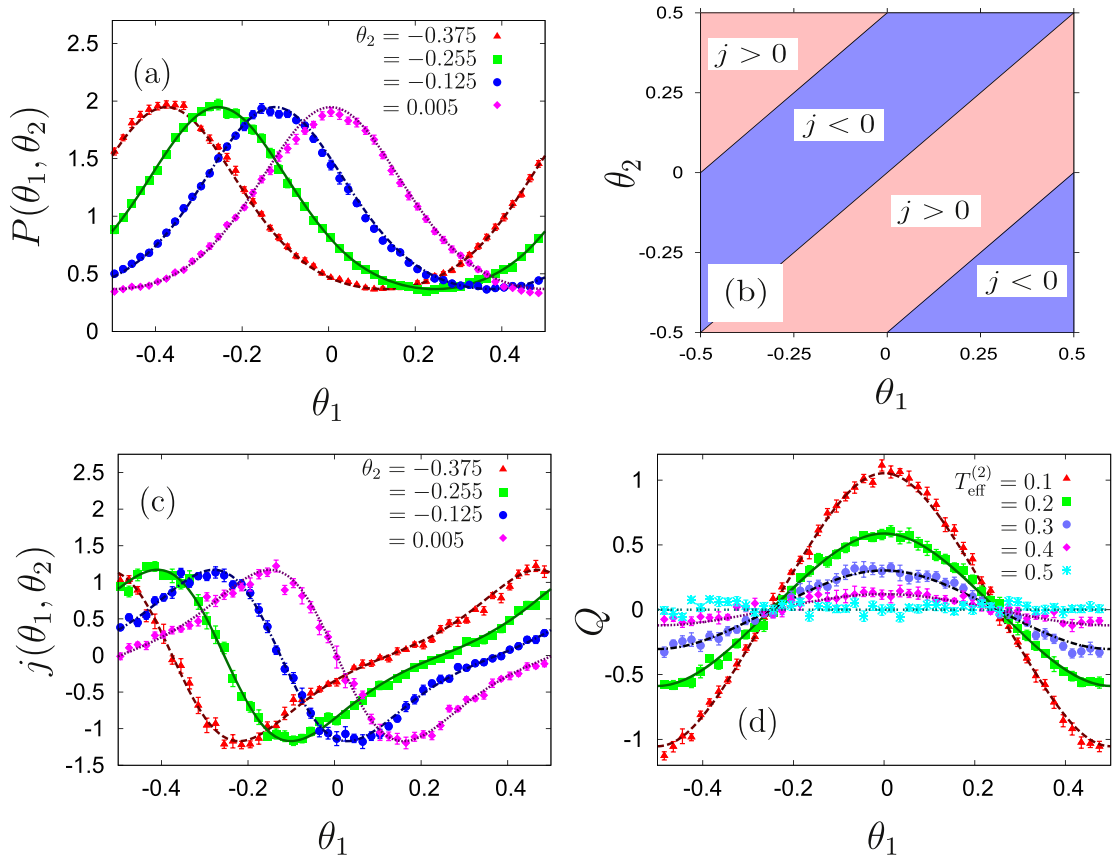

Figure 2. Ensemble-versus time-averaged properties. Panel (a): the pdf $P(\theta_1, \theta_2)$ as a function of θ_1 for four values of θ_2. The coupling parameter is $\varepsilon = 0.5$ Hz, $T_{\rm eff}^{(1)} = 0.5$ Hz, and $T_{\rm eff}^{(2)} = 0.1$ Hz, consistent with the observations made in [14, 20]. The curves correspond to the analytical prediction made in equation (3). The symbols represent the results of the numerical simulations (see section 3), based on a single-realization, time-averaged $P_{\mathcal{S}}(\theta_1, \theta_2)$ (equation (12)) with $\mathcal{S} = 10^4$ s (such that for a typical value of the frequency $\nu \simeq 47$ Hz [14], each flagella makes, on average, 4.7×10^5 full beats). Panel (b): sign of the out-of-equilibrium current $j(\theta_1, \theta_2)$ (equation (5)), which causes synchronized 'drifts' of phases $\theta_1(t)$ and $\theta_2(t)$, on the periodic (θ_1, θ_2)-plane for $T_{\rm eff}^{(1)} > T_{\rm eff}^{(2)}$. The black lines $\theta_1 = \theta_2$ and $|\theta_1 - \theta_2| = 1/2$ correspond to a change of sign, i.e. $j(\theta_1, \theta_2) = 0$. Panel (c): the out-of-equilibrium current $j(\theta_1, \theta_2)$ as a function of θ_1 for four values of θ_2. The coupling parameter is $\varepsilon = 0.5$ Hz, $T_{\rm eff}^{(1)} = 0.5$ Hz, and $T_{\rm eff}^{(2)} = 0.1$ Hz. The curves correspond to the analytical prediction made in equation (5). The symbols represent the results of numerical simulations for a single-realization time-averaged current $j_{\mathcal{S}}(\theta_1, \theta_2)$ in equation (13) with $\mathcal{S} = 10^6$ s. Panel (d): dimensionless order parameter Q as a function of θ_1 for $T_{\rm eff}^{(1)} = 0.5$ Hz, coupling parameter $\varepsilon = 0.5$ Hz, and five values of $T_{\rm eff}^{(2)}$. The curves correspond to the analytical prediction made in equation (7), which defines the ensemble-averaged order parameter Q. The symbols represent the results of the numerical simulations for the time-averaged order parameter $Q_{\mathcal{S}}$ (equation (14)), based on a single realization of the noises with $\mathcal{S} = 10^4$ s (i.e. approximately 2.8 h). Note that for $T_{\rm eff}^{(2)} = 0.5$ Hz, i.e. in the case of equal effective temperatures, both the ensemble-averaged order parameter Q and its time-averaged counterpart $Q_{\mathcal{S}}$ are equal to zero.

given by $Z = I_0(\varepsilon/(2\overline{T}_{\rm eff}))$, where $I_0(x)$ is a modified Bessel function of the first kind. We note that equation (3) here represents a particular case of a more general result derived in [28].

Since both natural frequencies ν_1 and ν_2 are taken to be equal, the steady-state solution $P(\theta_1, \theta_2)$ depends on the phases only via the phase difference, and thus becomes independent of $\nu = \nu_1 = \nu_2$ (see equation (3)). At first glance, the latter property appears to be somewhat astonishing, but it can be readily understood once one notices that the time evolution of the phase difference in the Langevin equations (1) becomes independent of ν if both natural frequencies are equal to each other. This means that $P(\theta_1, \theta_2)$ is defined in the frame of reference rotating with the unique frequency ν. Naturally, the maximum of $P(\theta_1, \theta_2)$ occurs for $\theta_1 = \theta_2$, regardless of the relation between the temperatures $T_{\rm eff}^{(1)}$ and $T_{\rm eff}^{(2)}$. For $\varepsilon/(2\overline{T}_{\rm eff}) \to \infty$, the pdf turns into a delta function of the difference $\theta_1 - \theta_2$. Figure 2(a) provides the pdf $P(\theta_1, \theta_2)$ (equation (3)) as a function of θ_1 for several fixed values of θ_2.

2.1.2. Out-of-equilibrium current

A remarkable feature of the minimal model with two different temperatures is, that in the non-equilibrium steady-state a nonzero current **J** occurs. This is a well-known aspect for stochastic dynamics of coupled components, each evolving at its own temperature (see, e.g. [26–33]). However, in the case at hand this nonzero current has a peculiar form due to the fact that the coupling term in equation (1) is a periodic function of the phase difference. The components J_1 and J_2 of this current can be inferred directly from the Fokker–Planck

equation (A1) (see appendix, equation (A2)). They obey

$$J_1 = J_2 = j(\theta_1, \theta_2) + \nu P(\theta_1, \theta_2). \tag{4}$$

The expression on the right-hand side (rhs) of equation (4) contains the trivial term $\nu P(\theta_1, \theta_2)$, which is the same for both components as could be expected on general grounds. It appears due to the constant drift term $\nu = \nu_1 = \nu_2$ on the rhs of the Langevin equations (1). In addition, there is a non-trivial contribution $j(\theta_1, \theta_2)$, which is a steady-state current in the frame rotating with the unique frequency ν; it reads

$$j(\theta_1, \theta_2) = -\pi\varepsilon \frac{\Delta T_{\rm eff}}{2\overline{T}_{\rm eff}} \sin(2\pi(\theta_2 - \theta_1)) P(\theta_1, \theta_2), \tag{5}$$

with $\Delta T_{\rm eff} = T^{(1)}_{\rm eff} - T^{(2)}_{\rm eff}$. Rather unexpectedly, $j(\theta_1, \theta_2)$ appears also to be the *same* for both components J_1 and J_2 of the current $\mathbf{J}$, due to the form of the pdf in equation (3).

The mean out-of-equilibrium current

$$\langle j(\theta_1, \theta_2)\rangle \equiv \int_{-1/2}^{1/2}\int_{-1/2}^{1/2} {\rm d}\theta_1 {\rm d}\theta_2\, j(\theta_1, \theta_2) = 0, \tag{6}$$

vanishes such that, due to $\langle P(\theta_1, \theta_2)\rangle = 1$, $\langle J_1\rangle = \langle J_2\rangle = \nu$. One can straightforwardly check that $\int_{-1/2}^{1/2} {\rm d}\theta_1 j(\theta_1, \theta_2) = 0 = \int_{-1/2}^{1/2} {\rm d}\theta_2 j(\theta_1, \theta_2)$. On the other hand, $j(\theta_1, \theta_2)$ is not equal to zero locally (except for $\theta_1 = \theta_2$ and $|\theta_1 - \theta_2| = 1/2$, where the current changes sign), and its sign and amplitude depend on the precise values of the phases θ_1 and θ_2. In figure 2(b), for a particular example with $T^{(1)}_{\rm eff} > T^{(2)}_{\rm eff}$, we present a 'phase chart' for the sign (i.e. the direction) of the out-of-equilibrium current $j(\theta_1, \theta_2)$ in the periodic (θ_1, θ_2)-plane. Further on, in figure 2(c) we show the current $j(\theta_1, \theta_2)$ (equation (5)) as a function of θ_1 for several fixed values of θ_2, which also provides insight into its amplitude.

2.1.3. Out-of-equilibrium synchronization

Equations (4) and (5) demonstrate that in a minimal model with two different effective temperatures, in addition to a stochastic phase locking of the coupled phases θ_1 and θ_2 (as observed in [14]), there is a different synchronization mechanism (based on the out-of-equilibrium current $j(\theta_1, \theta_2)$) which manifests itself via drifts of the phases. These drifts are correlated in that they have the same sign (i.e. direction) and the same amplitude for both phases. The actual direction of such drifts depends on the sign of $\Delta T_{\rm eff}$, as well as on the relative positions of θ_1 and θ_2 with respect to each other. In order to illustrate this behavior, we suppose $\Delta T_{\rm eff} > 0$ and $0 < \theta_2 - \theta_1 < 1/2$. In this case, according to equation (5), both θ_1 and θ_2 experience a drift in the negative direction up to the time at which, due to the thermal noise, the phase difference exceeds the value $1/2$ so that $\theta_2 - \theta_1 > 1/2$. Then, both θ_1 and θ_2 revert the direction of their drift. Once θ_1 and θ_2 interchange their positions, such that $-1/2 < \theta_2 - \theta_1 < 0$, the current $j(\theta_1, \theta_2)$ changes sign and turns positive, so that both θ_1 and θ_2 drift in the positive direction. Once $\theta_2 - \theta_1 < -1/2$, the drift direction again changes sign and becomes negative.

2.1.4. An order parameter in the steady-state

In order to quantify this novel synchronization mechanism, and also in order to render it observable either experimentally or in numerical simulations, one has to introduce a meaningful order parameter. In view of the above discussion, for a minimal model with two effective temperatures the latter should be associated with the steady-state current $j(\theta_1, \theta_2)$. As in general, there is, however, some liberty in choosing this parameter. Here we define an order parameter by integrating the out-of-equilibrium current $j(\theta_1, \theta_2)$ over θ_2 across half of the domain in which this variable is defined, and dividing the result by the mean effective temperature. This gives the following *dimensionless* order parameter (see equations (3) and (5))

$$\begin{aligned} Q(\theta_1) &= \frac{1}{\overline{T}_{\rm eff}} \int_0^{1/2} {\rm d}\theta_2\, j(\theta_1, \theta_2) \\ &= \frac{\Delta T_{\rm eff}}{\overline{T}_{\rm eff}} \frac{\sinh((\varepsilon/(2\overline{T}_{\rm eff})\cos(2\pi\theta_1))}{I_0(\varepsilon/(2\overline{T}_{\rm eff}))}. \end{aligned} \tag{7}$$

This order parameter Q is a function of the phase θ_1 and depends on the coupling parameter ε as well as on the values of the effective temperatures. It vanishes for $\varepsilon \to 0$, for $\overline{T}_{\rm eff} \to \infty$, and for $T^{(1)}_{\rm eff} \to T^{(2)}_{\rm eff}$, the latter limit being characteristic of the transition to the equilibrium setup. The order parameter also vanishes for $\theta_1 = \pm\pi/4$.

It is rewarding to determine the asymptotic behavior of Q in several particular limits. For instance, in the high-temperature limit one has

$$Q(\theta_1) \simeq \frac{\Delta T_{\rm eff}}{2\overline{T}_{\rm eff}^2}\varepsilon\cos(2\pi\theta_1),\ \overline{T}_{\rm eff} \gg \varepsilon/2, \tag{8}$$

which reduces to

$$Q(\theta_1) \simeq \frac{2\ \mathrm{sign}(T_{\rm eff}^{(1)} - T_{\rm eff}^{(2)})}{\max(T_{\rm eff}^{(1)},\ T_{\rm eff}^{(2)})}\ \varepsilon\cos(2\pi\theta_1), \tag{9}$$

if one of the effective temperatures is much higher than the other one.

In the opposite limit $\overline{T}_{\rm eff} \ll (\varepsilon\cos(2\pi\theta_1))/2$, which can be reached either via a sufficiently strong coupling ε (and for such values of θ_1 for which $\cos(2\pi\theta_1)$ is nonzero) or if both temperatures are sufficiently small. In these cases the system is close to the realm of the standard noiseless Kuramoto model and one finds directly from equation (7) that, in leading order in the parameter $\varepsilon/(2\overline{T}_{\rm eff}) \to \infty$, the order parameter Q varies as

$$Q(\theta_1) \simeq \frac{\Delta T_{\rm eff}}{2\overline{T}_{\rm eff}^{3/2}}(\pi\varepsilon)^{1/2}\exp\left(-\frac{\varepsilon}{\overline{T}_{\rm eff}}\sin^2(\pi\theta_1)\right). \tag{10}$$

In these limits $T_{\rm eff}^{(1,2)} \to 0$ and for any $\theta_1 \neq 0$, $Q(\theta_1)$ is exponentially small. For $\theta_1 = 0$, the exponential factor in the latter expression equals 1 and hence the order parameter Q varies algebraically as function of the effective temperatures and the coupling parameter ε:

$$Q(\theta_1 = 0) \simeq \frac{\Delta T_{\rm eff}(\pi\varepsilon)^{1/2}}{2\overline{T}_{\rm eff}^{3/2}}, \tag{11}$$

i.e. it is a non-analytic function of the coupling parameter and the effective temperatures.

2.2. Time-averaged properties for individual realizations of noises

It is not always possible to generate a statistical sample of large enough size, either in experiments or in numerical simulations, which allows one to average over an ensemble of trajectories. To this end, we present alternative definitions for the pdf $P(\theta_1, \theta_2)$, the current $j(\theta_1, \theta_1)$, and the order parameter Q, based on their time-averaged counterparts.

2.2.1. The pdf for a single realization of noises

The pdf $P(\theta_1, \theta_2)$ (equation (3)) obeys $P(\theta_1,\ \theta_2) = \lim_{\mathcal{S}\to\infty} P_{\mathcal{S}}(\theta_1,\ \theta_2)$ with

$$P_{\mathcal{S}}(\theta_1,\ \theta_2) = \frac{1}{\mathcal{S}}\int_0^{\mathcal{S}} \mathrm{d}t\ \delta(\theta_1(t) - \theta_1)\delta(\theta_2(t) - \theta_2), \tag{12}$$

where $\theta_1(t)$ and $\theta_2(t)$ are two individual realizations of the trajectories of the phases, corresponding to the solutions of the Langevin equations (equation (1)) for a given realization of the noises $\zeta_1(t)$ and $\zeta_2(t)$ in equation (2). In equation (12), $P_{\mathcal{S}}(\theta_1,\ \theta_2)$ is the total number of simultaneous occurrences, within the time interval $(0,\ \mathcal{S})$, of two given realizations of the trajectories $\theta_1(t)$ and $\theta_2(t)$ at the positions θ_1 and θ_2, respectively, divided by the observation time $\mathcal{S}$. If the system under study is ergodic, as it is the case (see section 3), the ensemble average and the time average yield identical results, such that, in the limit $\mathcal{S} \to \infty$, $P_{\mathcal{S}}(\theta_1,\ \theta_2)$ should attain $P(\theta_1, \theta_2)$.

2.2.2. Time-averaged current

We introduce the current $j_{\mathcal{S}}(\theta_1,\ \theta_2)$ as an average over the observation time $\mathcal{S}$:

$$\begin{aligned} j_{\mathcal{S}}(\theta_1,\ \theta_2) &= -\frac{1}{\mathcal{S}}\int_0^{\mathcal{S}} \mathrm{d}t\ \dot{\theta}_1(t)\delta(\theta_1(t) - \theta_1)\delta(\theta_2(t) - \theta_2) \\ &= -\frac{1}{\mathcal{S}}\int_0^{\mathcal{S}} \mathrm{d}t\ \dot{\theta}_2(t)\delta(\theta_1(t) - \theta_1)\delta(\theta_2(t) - \theta_2), \end{aligned} \tag{13}$$

where $\theta_1(t)$ and $\theta_2(t)$ obey equation (1) with ν set to zero. Note that the expressions in the first and the second line in equation (13) correspond to the components of the current $\mathbf{J}$ and differ with respect to the time derivative of the phases, i.e. $\dot{\theta}_1(t)$ or $\dot{\theta}_2(t)$. As we have shown above, the components of the ensemble-averaged current are exactly equal to each other. We thus expect (and verify via numerical simulations) that the same holds for their introduced time-averaged counterparts.

2.2.3. Time-averaged order parameter $Q_{\mathcal{S}}$

We integrate the expression in the first line on the rhs of equation (13) over θ_2 across one half of the domain in which this variable is defined. Dividing the result by the mean effective temperature (see the definition of Q in equation (7)), we obtain

$$Q_{\mathcal{S}} = -\frac{1}{\mathcal{S}\overline{T}_{\rm eff}}\int_0^{\mathcal{S}} {\rm d}t\ \dot{\theta}_1(t)\delta(\theta_1(t)-\theta_1)\times\int_0^{1/2}{\rm d}\theta_2\ \delta(\theta_2(t)-\theta_2)$$
$$= -\frac{1}{\mathcal{S}\overline{T}_{\rm eff}}\int_0^{\mathcal{S}} {\rm d}t\ \dot{\theta}_1(t)\delta(\theta_1(t)-\theta_1)\theta_{\rm H}(\theta_2(t)), \qquad (14)$$

where $\theta_{\rm H}(z)$ is the Heaviside theta-function, which is zero for $z<0$ and 1 for $z>0$. We expect that, similarly to the time-averaged quantity $P_{\mathcal{S}}(\theta_1,\ \theta_2)$ (equation (12)) and to the time-averaged current in equation (13), for large observation times $\mathcal{S}\to\infty$, $Q_{\mathcal{S}}$ converges to Q given in equation (7).

3. Discussion

In figure 1 we present appropriately discretized, individual realizations of the trajectories $\theta_1(t)$ and $\theta_2(t)$ which consist of $n=10^6$ steps with a discrete time step $\delta t=10^{-6}$ s (see the appendix for more details) for two distinct values of the coupling parameter ($\varepsilon=0.5$ Hz for the upper row and $\varepsilon=1$ Hz for the lower row), for the fixed effective temperature $T_{\rm eff}^{(1)}=0.5$ Hz of flagellum 1, and for three temperatures of flagellum 2 ($T_{\rm eff}^{(2)}=0,\ 0.1$, and 0.5 Hz). The case $T_{\rm eff}^{(2)}=0.5$ Hz, i.e. $T_{\rm eff}^{(1)}=T_{\rm eff}^{(2)}$ corresponds to the original one considered in [14]. In contrast, the trajectories in panels (a) and (d) of figure 1 correspond, within the present choices, to the extreme case of maximal disparity between the temperatures. In (a), $\theta_2(t)$ corresponds to zero temperature (i.e. a perfect rotary motor operating with no noise) and is entrained in random motion by $\theta_1(t)$, which is subject to random noise. Interestingly, the stochastic phase locking described in [14] is seemingly strongest in the case of equal temperatures (panels (c) and (f)), is less pronounced for the combination $T_{\rm eff}^{(1)}=0.5$Hz and $T_{\rm eff}^{(2)}=0.1$ Hz (panels (b) and (e)) and it is weakest for $T_{\rm eff}^{(1)}=0.5$ Hz and $T_{\rm eff}^{(2)}=0$ (panels (a) and (d)) for which the periods of synchrony are hardly visible. Therefore, the synchronization observed in [14] degrades if the effective temperatures become unequal.

The pdf $P(\theta_1,\theta_2)$ as a function of θ_1 for several values of θ_2 is illustrated in figure 2(a) together with the results of numerical simulations for the time-averaged, single-trajectory quantity $P_{\mathcal{S}}(\theta_1,\ \theta_2)$ in equation (12). The very nice agreement between $P(\theta_1,\theta_2)$ and $P_{\mathcal{S}}(\theta_1,\ \theta_2)$ shows indirectly that the system is indeed ergodic. Such an agreement is, however, achieved for trajectories which are substantially longer than the ones shown in figure 1. Here we have used the same $\delta t=10^{-6}$ s but a larger value $n=10^{10}$, so that the observation time is $\mathcal{S}=10^4$ s.

We use next the trajectories provided in figure 1 in order to obtain the introduced time-averaged current $j_{\mathcal{S}}(\theta_1,\ \theta_2)$ (equation (13)) for individual realizations of $\theta_1(t)$ and $\theta_2(t)$. The results (see the appendix for more details) are presented in figure 2(c) together with the ensemble-average of $j(\theta_1,\theta_2)$ (equation (5)) as obtained from the solution of the Fokker–Planck equation. The agreement between the two results is very satisfactory for $n=10^{12}$ and $\delta t=10^{-6}$ s, such that the observation time $\mathcal{S}=10^6$ s. For smaller n the data appear more noisy and no conclusive statement on the convergence of $j_{\mathcal{S}}(\theta_1,\ \theta_2)$ to $j(\theta_1,\theta_2)$ can be made.

In figure 2(d) we show Q obtained from equation (7) together with $Q_{\mathcal{S}}$ following from equation (14). The latter is obtained from the trajectories depicted in figure 1 (with $\delta t=10^{-6}$ and $n=10^{10}$, such that $\mathcal{S}=10^4$ s), as function of θ_1 for $\varepsilon=0.5$ Hz, $T_{\rm eff}^{(1)}=0.5$ Hz, and three values of $T_{\rm eff}^{(2)}$. We observe full agreement between our theoretical prediction in equation (7), which is defined for an ensemble of trajectories, and $Q_{\mathcal{S}}$ as introduced in equation (14), which is defined for a single realization of noises. This implies that the latter can be conveniently used for a single-trajectory analysis of corresponding experimental and numerical data. Finally, we note that a rather long observation time $\mathcal{S}=10^4$ s has been used in figure 2(d) in order to demonstrate convergence of the time-averaged order parameter to the ensemble-averaged one. The observation that the order parameter $Q_{\mathcal{S}}$ deviates from zero in out-of-equilibrium conditions can be made already for more moderate values of n, although the data will look more noisy.

In summary, we have presented a generalization of a minimal model introduced in [14] to the case in which the phases in equation (1) are subject to noises with different amplitudes. This can be thought of as a noisy Kuramoto (or Sakaguchi) model of two coupled oscillators with distinct effective temperatures. From a physical point of view, the original model in [14] has been introduced in order to describe the noisy synchronization of two identical flagella of a biflagellate alga. Our generalized model is expected to be appropriate for the description of a noisy synchronization of two flagella having different lengths. Indeed, the analysis in [20] has revealed that the noise amplitudes depend on the length of the flagella. Viewed from a different perspective, our study provides an, apparently first, solvable example for the synchronization of coupled oscillators under out-of-equilibrium conditions. Hence, it opens new perspectives for a similar analysis of more complicated models, such as a FitzHugh–Nagumo model (see, e.g. [24]). Note that in the example studied here the difference between the effective temperatures is not artificially imposed but emerges naturally.

We have shown, both analytically and numerically, that in such a system a very peculiar form of a synchronization of two coupled oscillators takes place. It is mediated by an emerging, current-carrying steady-state. More specifically, we have shown that, on top of the synchronization of the phases as observed in [14], i.e. a

stochastic phase locking, an additional synchronized rotation (drifts) of the phases takes place. In order to quantify the degree of such a synchronization, we have introduced a characteristic order parameter, which vanishes if the effective temperatures become equal to each other. This order parameter has been determined as the average over an ensemble of realizations of the stochastic evolution of phases, as well as on the level of an individual realization. The latter makes the order parameter suitable for experimental and numerical analyses, for which a sufficiently large statistical sample cannot be formed. Via numerical simulations we have shown that both definitions become equivalent in the limit of sufficiently long observation times, which also demonstrates the ergodicity of the system under study. Finally, we remark that we expect a much richer behavior for the relevant situation in which, in addition to unequal effective temperatures, the natural frequencies are also different. This is a challenging subject for future research.

Acknowledgments

The authors acknowledge valuable discussions with M Dykman, F Ritort, M Rosenblum, and S Ruffo. The work by AM has been partially supported by the Polish National Science Center (Harmonia Grant No. 2015/18/M/ST3/00403).

Appendix. Details of calculations

A.1. Analytical approach

We provide the Fokker–Planck equation for the joint pdf $P(\theta_1, \theta_2)$, associated with the system of two coupled Langevin equations (equation (1)) with the noise terms defined by equation (2). The associated Fokker–Planck equation is derived by standard means [15] and reads

$$\begin{aligned}\dot{P}(\theta_1,\,\theta_2) &= -\mathrm{div}\,\mathbf{J} = -\frac{\partial}{\partial\theta_1}J_1 \;-\; \frac{\partial}{\partial\theta_2}J_2 \\ &= \left(\frac{\partial}{\partial\theta_1}\left[T_{\mathrm{eff}}^{(1)}\frac{\partial}{\partial\theta_1} + (\pi\varepsilon\sin(2\pi(\theta_1-\theta_2)) - \nu)\right]\right. \\ &\quad \left. + \frac{\partial}{\partial\theta_2}\left[T_{\mathrm{eff}}^{(2)}\frac{\partial}{\partial\theta_2} - (\pi\varepsilon\sin(2\pi(\theta_1-\theta_2)) + \nu)\right]\right)P(\theta_1,\,\theta_2),\end{aligned} \tag{A1}$$

where $\mathbf{J} = (J_1, J_2)$ is the probability current. The steady-state solution of equation (A1) can be determined analytically and is given by equation (3) in section 2.

From equation (A1) we infer the following expressions for the components J_1 and J_2 of the out-of-equilibrium current $\mathbf{J}$:

$$\begin{aligned}J_1 &= -\left(T_{\mathrm{eff}}^{(1)}\frac{\partial}{\partial\theta_1} + (\pi\varepsilon\sin(2\pi(\theta_1-\theta_2)) - \nu)\right)P(\theta_1,\,\theta_2) \\ J_2 &= -\left(T_{\mathrm{eff}}^{(2)}\frac{\partial}{\partial\theta_2} - (\pi\varepsilon\sin(2\pi(\theta_1-\theta_2)) + \nu)\right)P(\theta_1,\,\theta_2).\end{aligned} \tag{A2}$$

Inserting the explicit expression of the pdf in equation (3) into (A2), and performing differentiations, we obtain equation (4).

Rewriting the components J_1 and J_2 of the out-of-equilibrium current $\mathbf{J}$ in that frame of reference which rotates with the frequency ν, for $j(\theta_1, \theta_2)$ (see the definition in equation (5)) we find

$$\begin{aligned}j(\theta_1,\,\theta_2) &= -\left(T_{\mathrm{eff}}^{(1)}\frac{\partial}{\partial\theta_1} + \pi\varepsilon\sin(2\pi(\theta_1-\theta_2))\right)P(\theta_1,\,\theta_2) \\ &= -\left(T_{\mathrm{eff}}^{(2)}\frac{\partial}{\partial\theta_2} - \pi\varepsilon\sin(2\pi(\theta_1-\theta_2))\right)P(\theta_1,\,\theta_2). \\ &= -\pi\varepsilon\frac{\Delta T_{\mathrm{eff}}}{2\overline{T}_{\mathrm{eff}}}\sin(2\pi(\theta_2-\theta_1))P(\theta_1,\,\theta_2).\end{aligned} \tag{A3}$$

The expression in the last line in equation (A3) corresponds to our equation (5).

A.2. Numerical approach

Here, we provide a brief description of our numerical algorithm. To this end we rewrite the Langevin equations (equation (1)) in the frame of reference rotating with the frequency ν, i.e. we change variables according to $\theta_{1,2} = \tilde{\theta}_{1,2}(t) + \nu t$, and then we discretize the time variable $t = n\delta t$, where n is an integer; δt is the time-interval

between the consecutive steps. Without loosing generality, in what follows we set $\nu = 0$ and, in order to avoid a clumsy notation, we drop the tilde mark. Lastly, we recall the standard scaling properties of Gaussian delta-correlated noises $\zeta_{1,2}(t)$ in order to cast the noise terms into a different (but equivalent) form, in which the effective temperatures appear explicitly as amplitudes of the noises [15]. This turns equation (1) into recurrence relations of the form

$$\theta_1(t+\delta t) = \theta_1(t) - \delta t\left(\pi\varepsilon \sin\left[2\pi\Delta_t\right] + \sqrt{\frac{2T_{\rm eff}^{(1)}}{\delta t}}\,\eta_1(t)\right),$$
$$\theta_2(t+\delta t) = \theta_2(t) + \delta t\left(\pi\varepsilon \sin\left[2\pi\Delta_t\right] + \sqrt{\frac{2T_{\rm eff}^{(2)}}{\delta t}}\,\eta_2(t)\right), \tag{A4}$$

where $\Delta_t = \theta_1(t) - \theta_2(t)$ is an instantaneous phase difference. The above recursions (with dimensionless prefactors of the sine and of the noise terms) allow us to define the values of $\theta_1(t+\delta t)$ and $\theta_2(t+\delta t)$ through the values of Δ_t and the values of the noise terms $\eta_{1,2}(t)$ at the previous moment of time. This permits us to sequentially generate individual realizations of the phases $\theta_1(t)$ and $\theta_2(t)$ of arbitrary duration t. The noises $\eta_1(t)$ and $\eta_2(t)$ in equation (A4) are dimensionless Gaussian random variables, uncorrelated for distinct values of n, with zero mean and variances $\sigma_{1,2}^2 \equiv 1$, such that the pdf is given explicitly by $P(\eta_{1,2}) = \exp(-\eta_{1,2}^2/2)/\sqrt{2\pi}$. This choice ensures that for $\varepsilon = 0$ the phases $\theta_1(t)$ and $\theta_2(t)$ undergo standard diffusive motion on the unit circle with diffusion coefficients $T_{\rm eff}^{(1)}$ and $T_{\rm eff}^{(2)}$, respectively.

Adopting $\delta t = 10^{-6}$ s (which is sufficiently short such that for a typical beating frequency of $\nu \simeq 47$ Hz (see [14]) each flagella makes a full beat within roughly 2.13×10^4 intervals δt), we generate two individual realizations of noises, thereby building up individual realizations of the trajectories $\theta_1(t)$ and $\theta_2(t)$ which consist of $n = 10^6$ steps. As a consequence, within the full observation time (here $\mathcal{S} = 1$ s) each flagella makes, on average, 47 full beats. These trajectories are depicted in figure 1.

In order to determine numerically the introduced time-averaged current $j_{\mathcal{S}}(\theta_1, \theta_2)$ (equation (13)) for individual realizations of $\theta_1(t)$ and $\theta_2(t)$, we first appropriately discretize the expression on the rhs of equation (13) and replace the time-derivative $\dot{\theta}_1(t)$ (or $\dot{\theta}_2(t)$) by the finite difference given by equation (A4). Then, we use the trajectories provided in figure 1. The results of such a procedure are presented in figure 2(c) together with the ensemble-average of $j(\theta_1, \theta_2)$ (equation (5)) as obtained from the solution of the Fokker–Planck equation. The order parameter $Q_{\mathcal{S}}$, as introduced in equation (14), is determined numerically in a similar way.

ORCID iDs

A Maciolek https://orcid.org/0000-0002-2371-4183
G Oshanin https://orcid.org/0000-0001-8467-3226

References

[1] Polin M, Tuval I, Drescher K, Gollub J P and Goldstein R E 2009 Chlamydomonas swims with two 'gears' in a eukaryotic version of run-and-tumble locomotion *Science* **325** 487
[2] Strogatz S H 2000 From Kuramoto to Crawford: exploring the onset of synchronization in populations of coupled oscillators *Physica* D **143** 1
[3] Pikovsky A, Rosenblum M and Kurths J 2003 *Synchronization: A universal Concept in Nonlinear Sciences* (Cambridge: Cambridge University Press)
[4] Acebrón J A, Bonilla L L, Pérez Vicente C J, Ritort F and Spigler R 2005 The Kuramoto model: a simple paradigm for synchronization phenomena *Rev. Mod. Phys.* **77** 137
[5] Gupta S, Campa A and Ruffo S 2018 *Statistical Physics of Synchronization* (Berlin: Springer)
[6] Taylor G I 1951 Analysis of the swimming of microscopic organisms *Proc. R. Soc.* A **209** 447
[7] Machin K E 1963 The control and synchronization of flagellar movement *Proc. R. Soc.* B **158** 88
[8] Cosentino Lagomarsino M, Jona P and Bassetti B 2003 Metachronal waves for deterministic switching two-state oscillators with hydrodynamic interaction *Phys. Rev.* E **68** 021908
[9] Lenz P and Ryskin A 2006 Collective effects in ciliar arrays *Phys. Biol.* **3** 285
[10] Gueron S and Levit-Gurevich K 1999 Energetic considerations of ciliary beating and the advantage of metachronal coordination *Proc. Natl Acad. Sci. USA* **96** 12240
[11] Vilfan A and Jülicher F 2006 Hydrodynamic low patterns and synchronization of beating cilia *Phys. Rev. Lett.* **96** 058102
[12] Guirao B and Joanny J F 2007 Spontaneous creation of macroscopic flow and metachronal waves in an array of cilia *Biophys. J.* **92** 1900
[13] Niedermayer T, Eckhardt B and Lenz P 2008 Synchronization, phase locking, and metachronal wave formation in ciliary chains *Chaos* **18** 037128
[14] Goldstein R E, Polin M and Tuval I 2009 Noise and synchronization in pairs of beating eukaryotic flagella *Phys. Rev. Lett.* **103** 168103
[15] Gardiner C W 1983 *Handbook of Stochastic Methods* (Berlin: Springer)
[16] Berg H C 2003 The rotary motor of bacterial flagella *Annu. Rev. Biochem.* **72** 19

[17] Ma R, Klindt G S, Riedel-Kruse I, Jülicher F and Friedrich B M 2014 Active phase and amplitude fluctuations of flaggelar beating *Phys. Rev. Lett.* **113** 048101
[18] Wan K Y and Goldstein R E 2016 Coordinated beating of algal flagella is mediated by basal coupling *Proc. Natl Acad. Sci. USA* **113** E2784
[19] Liu Y, Claydon R, Polin M and Brumley D R 2018 Transitions in synchronization states of model cilia through basal-connection coupling *J. R. Soc. Interface* **15** 20180450
[20] Goldstein R E, Polin M and Tuval I 2011 Emergence of synchronized beating during the regrowth of eukaryotic flagella *Phys. Rev. Lett.* **107** 148203
[21] Rosenbaum J L, Moulder J E and Ringo D L 1969 Flagellar elongation and shortening in Chlamydomonas *J. Cell. Biol.* **41** 600
[22] Wilson N F, Iyer J K, Buchheim J A and Meek W 2008 Regulation of flagellar length in Chlamydomonas *Semin. Cell Developmental Biol.* **19** 494
[23] Malakhov A 1965 Influence of the intrinsic noise of oscillators on their mutual synchronization *Investiya VUZ Radiofiz.* **8** 1160
[24] Amro R M, Lindner B and Neiman A B 2015 Phase diffusion in unequally noisy coupled oscillators *Phys. Rev. Lett.* **115** 034101
[25] Sakaguchi H 1988 Cooperative phenomena in coupled oscillator systems under external fields *Prog. Theor. Phys.* **79** 39
[26] Filliger R and Reimann P 2007 Brownian gyrator: a minimal heat engine on the nanoscale *Phys. Rev. Lett.* **99** 230602
[27] Dotsenko V, Maciolek A, Vasilyev O and Oshanin G 2013 Two-temperature Langevin dynamics in a parabolic potential *Phys. Rev.* E **87** 062130
[28] Grosberg A Y and Joanny J-F 2015 Nonequilibrium statistical mechanics of mixtures of particles in contact with different thermostats *Phys. Rev.* E **92** 032118
[29] Murashita Y and Esposito M 2016 Overdamped stochastic thermodynamics with multiple reservoirs *Phys. Rev.* E **94** 062148
[30] Ciliberto S 2017 Experiments in stochastic thermodynamics: short history and perspectives *Phys. Rev.* X **7** 021051
[31] Fogedby H C and Imparato A 2017 A minimal model of an autonomous thermal motor *Europhys. Lett.* **119** 50007
[32] Mancois V, Marcos B, Viot P and Wilkowski D 2018 Two-temperature Brownian dynamics of a particle in a confining potential *Phys. Rev.* E **97** 052121
[33] Cerasoli S, Dotsenko V, Oshanin G and Rondoni L 2018 Asymmetry relations and effective temperatures for biased Brownian gyrators *Phys. Rev.* E **98** 042149